

# Geant4 Simulations of GeGa module behaviour under Proton Irradiation

Christian Bongardo (INAF-OAP), Paola Andreani (INAF-OAT)

First Version

**Table of Contents**

<b>1</b>	<b>Related Documents</b>	<b>3</b>
<b>2</b>	<b>Aim of the Document</b>	<b>3</b>
<b>3</b>	<b>Test Specimen</b>	<b>3</b>
<b>4</b>	<b>The G4 Simulations</b>	<b>3</b>
4.1	The Geometry of the Ge:Ga module . . . . .	4
4.2	Thresholds . . . . .	4
4.3	The definition of a glitch . . . . .	9
4.4	The Geant4 results . . . . .	9
<b>5</b>	<b>Comparison with measurements</b>	<b>9</b>
5.1	Events and rates . . . . .	9
5.2	Deposited energy . . . . .	11
5.3	Boundary effect . . . . .	12
5.4	Cross-talks . . . . .	12
<b>6</b>	<b>Conclusions</b>	<b>13</b>

## 1 Related Documents

PACS-ME-TP-009, 2004, Katterloher R., Barl L., & Shubert J., *Test Plan and Procedures for Investigation of Glitch Event Rate during Proton Irradiation (Test Report)*

P1CC-KL-TN-011, 2005, Royer P. *CQM Proton Irradiation Test Analysis*

P1CC-KL-TN-013, 2005, Royer P. *CQM Proton Irradiation Test Noise Evolution*

Technical Note, 2004, draft 1, Santin G., *Herschel PACS Photo-conductor: Simulation of the Proton Ground tests*

P1CC-KL-TN-012, 2005, Groenewegen M. *UCL-CRC Proton Tests of March 2004: glitch height distribution*

## 2 Aim of the Document

In this document we report on simulations, performed with the Geant4 code, of proton impact on a Ge:Ga module of the HERSCHEL/PACS Instrument. Simulations are built to reproduce the instrumental setup as it is described in [2] and results are compared with measurements outcomes.

**In particular in this draft we show comparison of simulated results with (a) the number and rates of detected events, (b) deposited energy on each pixel, (c) effects related to the geometry of the module, (d) effects on nearby pixels (cross-talks).**

The PACS CQM Spectrometer Module was tested under proton irradiation at the Light Ion Facility of the Centre de Recherches du Cyclotron of the University Catholique de Louvain La Neuve (UCL-CRC), Belgium, on March 4th and 6th 2004. Details of the instrument setup may be found in [2]. Tests aims are the determination of glitch event rate and performance variation in the Ge:Ga photo-conductor module and the measurement results are reported in [3], [1] and [4].

## 3 Test Specimen

The test specimen foreseen for the proposed investigations under proton irradiation is the detector module FM#12 with a CRE of the Qualification Model type, mounted in the centre of the module. The detector is in the high stress configuration. The module stood in a liquid He dewar operating at a temperature of  $(1.85 \pm 0.05)$  K.

The proton beam, before reaching the Ge:Ga crystals elements penetrate three concentric cylinders of Al (called hereafter Al1, Al2 and Al3) and one made of Cu. Al1 is 6 mm thick and has an external radius of 14.15 cm; Al2 1.5 mm with an external radius of 12.4 cm; Al3 is 1.5 mm thick and has external radius of 11.4 cm. The Cu cylinder is 0.5 mm thick and has external radius of 10.5 cm. The module is placed inside a box of Al 4 mm thick (*Al case*) so that half the foreoptics stands outside of it (see Fig. 3). The module is not placed at the centre of the cylinders.

During the test a primary circular (10 cm  $\emptyset$ ) proton beam of 70 MeV was used, with a beam line consisting of 5.78 m between the diffusion foil and the Device Under Test (DUT). Before the beam reached the dewar it crossed at least one layer of polystyrene ( $C_8H_8$ )<sub>n</sub>, whose position and thickness were not known. From the Technical Note of Santin ([5]) we argued such a layer may be 5 mm thick, but still its positioning<sup>1</sup> and density were not given<sup>2</sup>. The beam reaches the dewar (and the module) under an angle of 10°.

## 4 The G4 Simulations

We first run 5 simulations of 10000 protons each, in order to have an idea of what occurs to the beam once it crosses all the layers. We assume that the beam had a Gaussian error of 1 MeV. After the first layer of

<sup>1</sup>We supposed it being perpendicular to the beam. We placed it  $2R_{Al1}$  far from Al1 cylinder.

<sup>2</sup>We used 1.032 g/cm<sup>3</sup> (Particle Physics Booklet), but other texts report 1.05 g/cm<sup>3</sup>. Is that the right chemical composition of the polystyrene used (on a subsequent test they used a  $(C_{10}H_{11})_n$  scintillator)?

polystyrene we had an energy of  $\approx 64.98$  MeV, which is slightly higher than the SRIM computed value: 62.15 MeV [2]. This uncertainty may be due to our imperfect knowledge of the polystyrene layer thickness. On the other hand our simulations have been made considering that also the polystyrene foil is under vacuum while it was outside the dewar, i.e. in air. Air is a great energy leakage; it is fundamental to know how long is the path in air, where the polystyrene foil is placed, etc. In Fig. 1 we plotted the degradation of the proton energy along the tracking inside the dewar.

What we would like to stress here is that 10000 protons originate roughly 6800 secondary events. After the Al box, survive  $\approx 5100$  protons. But, after the Al box there are also  $\approx 1600$  secondary events. The spectral range and type of these secondary events is strictly dependent of the goodness on the models used in Geant4.

#### 4.1 The Geometry of the Ge:Ga module

The UCL-CRC investigation considered only one single module of the effective  $25 \times 16$  Ge:Ga photoconductor arrays. The detector material and amount of stress defines the wavelength range of the instrument. Light cones in front of the actual detector block provide area filling light collection in the focal plane feeding the light into the individual integrating cavities around each separate pixel. The detector crystals are connected to the input of the CRE (Cryogenic Readout Electronic). The high stressed module is cooled down to 1.8 K, the readout electronics (FEE) to 4 K.

All main metal components are made of a light metal alloy called Ergal.

The most important part of the photo-conductor is the cavity. The cavity is an empty box, of cylinder shape, whose major axis is displaced with respect to the major axis of the box.

Inside the cavity there is the active part: the pixel. Each pixel is made of Ge:Ga (in the high stress configuration Ga doping is  $10^{14} \text{ cm}^{-3}$ , that is an atom of Ga for about  $10^9$  atoms of Ge. We did not consider this low Ga concentration). The pixel is a simple box of  $1 \times 1 \times 1.5$  mm. Each pixel is sustained by two boxes (called hereafter cubes) made of CuBe2 (a Cu, Be and Pb alloy),  $0.94 \times 0.94 \times 0.3$  mm. Between two sequences of pixels there is an  $\text{Al}_2\text{O}_3$  (Aluminum oxide) insulator. It is a cylinder of 1.49 mm radius and 0.5 mm high. The sequence of the 16 pixels starts with an insulator and ends with a *kugel* (a steel cylinder). The pixels have a single face that is not shadowed by the cavity, that is, clearly, the one facing the fore optics.

The fore optics (hereafter FO) is the most difficult part to be designed with Geant4. Actually it is constructed as a unique block made of Ergal, from which they subtracted a cone non orthogonal to the respective pixel. We designed the cones one by one, making use of the boolean solids. All the FO should be gold coated with a 8.95 g gold mass. Simple calculations of the surface area of the FO leads to a coating thickness of  $\approx 1.6 \mu\text{m}$ : we did not reproduce such a coating.

The FEE is made of two different volumes: a box and a trapezoid. The box is  $48 \times 26 \times 0.5$  mm; the trapezoid has the same major base (48 mm, minor base 38 mm, height 5 mm) and thickness as the FEE. The FEE is coated with a  $10 \mu\text{m}$  layer of gold.

We won't describe every other single piece of the module. We only stress that the ergal components of the module have three different thicknesses. The small cubes sustaining the FO are 1.75 mm thick; the end of the horseshoe is 2.3 mm thick; the horseshoe is 4.1 mm thick.

#### 4.2 Thresholds

Each particle has an associated production threshold, i.e. either a distance, or a range cut-off, which is converted to an energy for each material, which should be defined as an external requirement. Fixing these thresholds is mandatory to avoid a too large unrealistic secondary production (infrared divergence).

We have set different production thresholds (hereafter cuts) for each geometrical region.

The G4 default values, 0.7mm, could force a too large production of secondary particles for those thick volumes and a too small production for thin regions. We first ran our G4 code with the default cut value of 0.7 mm for all volumes and then tuned them according to the module geometry. We identified groups of volumes with the

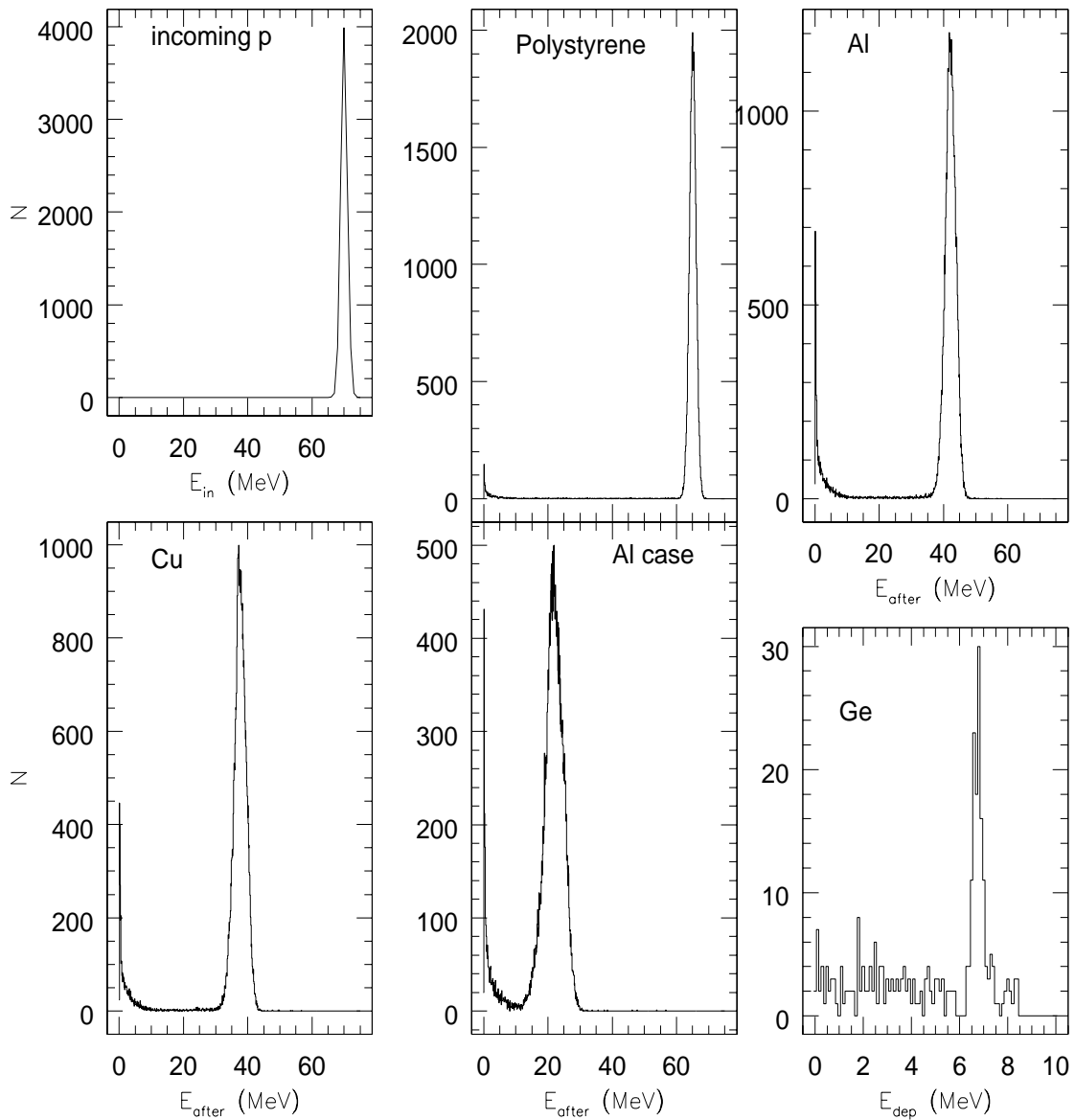


Figure 1: Degradation of the proton energy across the dewar layers: from the top-left panel, the energy of the incoming proton flux, the flux emerging from the polystyrene foil, after the Aluminum shields, after the Cu case and the final detector case. The last panel refers to the energy deposition on the Ge:Ga material.

Region	Cut Value	Thickness
Shield	2 mm	11 mm
High_mm	0.7 mm	3.02 - 4.1 mm
Low_mm	0.3 mm	0.73 - 2.1 mm
High_mic	100 $\mu\text{m}$	300 - 600 $\mu\text{m}$
Low_mic.a	5 $\mu\text{m}$	20 $\mu\text{m}$
Low_mic.b	3 $\mu\text{m}$	10 $\mu\text{m}$

Table 1: The six geometrical regions of the module and their specific cut values.

Exp.	BIAS (mV)	$t_{ramps}$ (ms)	C (pF)	$N_{ramps}$	$N_{rep}$	Flux ( $\text{cm}^{-2}\text{s}^{-1}$ )	E (MeV)
#N1	30	300	0.3	128	2	0.5	62.15
	30	300	0.1	128	2	0.5	62.15
	50	300	0.3	128	1	0.5	62.15
	70	1000	3.0	256	2	0.5	62.15
	70	300	1.0	512	1	0.5	62.15
	70	300	1.0	1024	1	0.5	62.15
	50	300	1.0	512	1	10.0	62.15
	50	300	3.0	512	44	10.0	62.15
	70	300	3.0	512	40	10.0	62.15
	70	300	3.0	1024	5	10.0	62.15
#N2	50	300	3.0	2048	3	10.0	62.15
	50	300	3.0	2048	2	10.0	62.15
	50	300	3.0	1024	1	10.0	62.15
	50	300	3.0	2048	2	10.0	62.15
	50	300	3.0	1024	1	10.0	62.15
	50	300	3.0	2048	2	10.0	62.15
	50	300	3.0	2048	3	10.0	62.15
	50	300	3.0	1024	1	10.0	62.15
	50	300	3.0	2048	2	10.0	62.15
	50	300	3.0	2048	3	10.0	62.15
#S1	50	300	3.0	512	1	400.0	62.15
	50	30	3.0	5000	1	400.0	62.15
	30	300	3.0	512	14	400.0	62.15
	50	300	3.0	2048	2	400.0	62.15
	50	100	3.0	2048	1	400.0	62.15
#S2	50	300	3.0	2048	1	400.0	59.84
	50	300	0.3	2048	1	400.0	59.84
	50	300	0.3	1024	1	400.0	59.84

Table 2: Summary of proton seed and photo-conductor module setup during UCL-CRC experiments. Column # 1 reports the identifier of the chosen setup, # 2 the value of the bias voltage of the FEE circuit, # 3 the duration of each integration ramp, # 4 the integrator capacitor, # 5 the number of ramps, # 6 the number of repetition with the same measurement setup, # 7 the proton flux, # 8 the proton energy as given by the SRIM software (see [2] and test for details).

same thicknesses: in particular we defined 6 different regions with rather the same thickness (see Table 1)<sup>3</sup>. Results are robust since they do not depend on the cut values, both default ones and the chosen ones lead to similar outputs, but a slight increasing of the secondary event production. On the one hand this was expected, since most of the volumes have still the same default cut value, 0.7 mm. On the other hand it is possible that Ergal thresholds have already achieved convergence at the default value, that is we are very slightly tuning them. Although results are pretty similar those with our chosen cuts allow a better tracking inside the sensitive detector volume.

In Tab. 2 the UCL-CRC experiment as performed at Louvain cyclotron [2].

The same standard 70 MeV proton beam was always used and the deposited energy on the module has been

<sup>3</sup>We decided not to use very small cut values (below 1-2  $\mu\text{m}$ ), since this could affect the validity of physical models at such small steps (Ivantchenko, private communication).

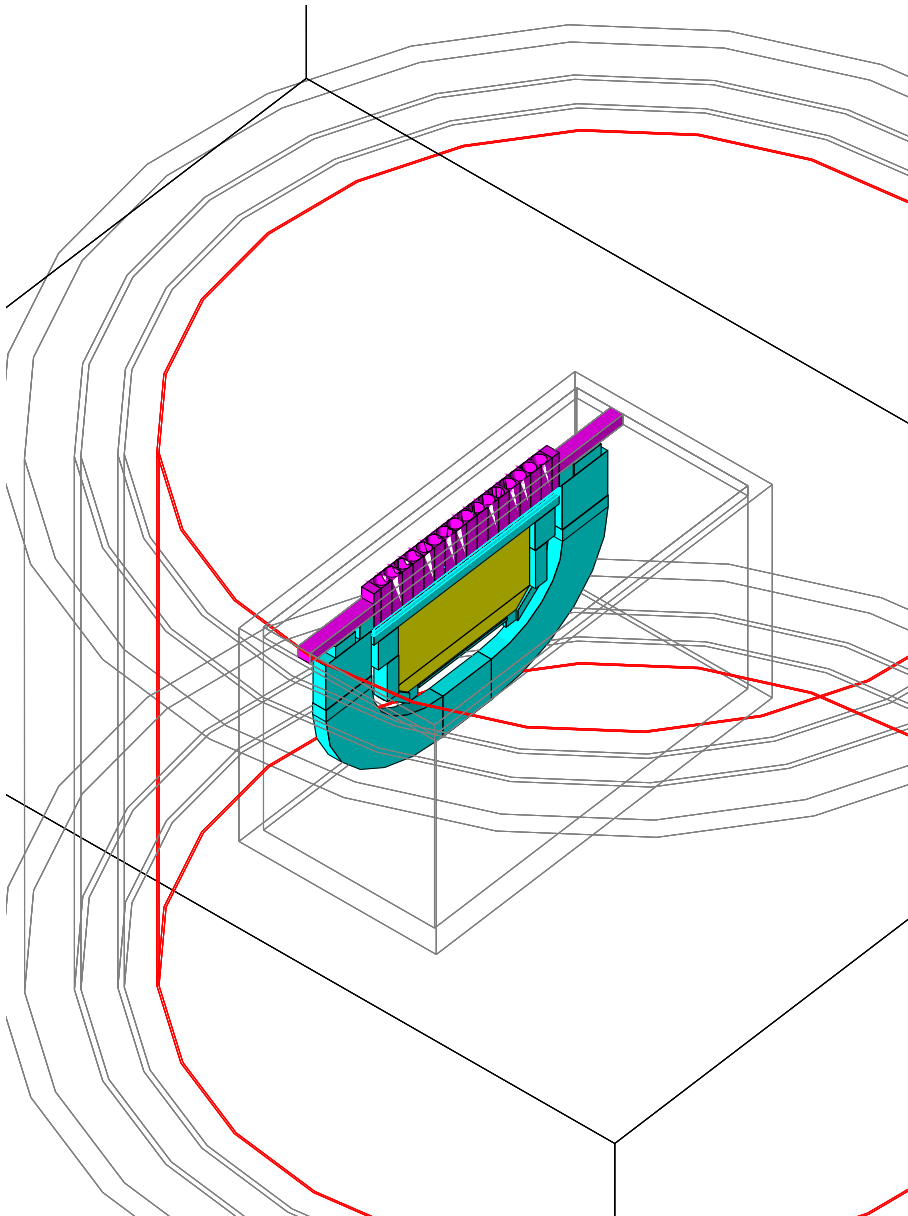


Figure 2: A single PACS high stress module, Magenta: the foreoptics, Yellow: the gold coating of the FEE and the active pixel. Red: the CuBe2 contacts. Blue: the Al<sub>2</sub>O<sub>3</sub> insulator. Gray: the cylindrical steel segment. Cyan: ergal components.

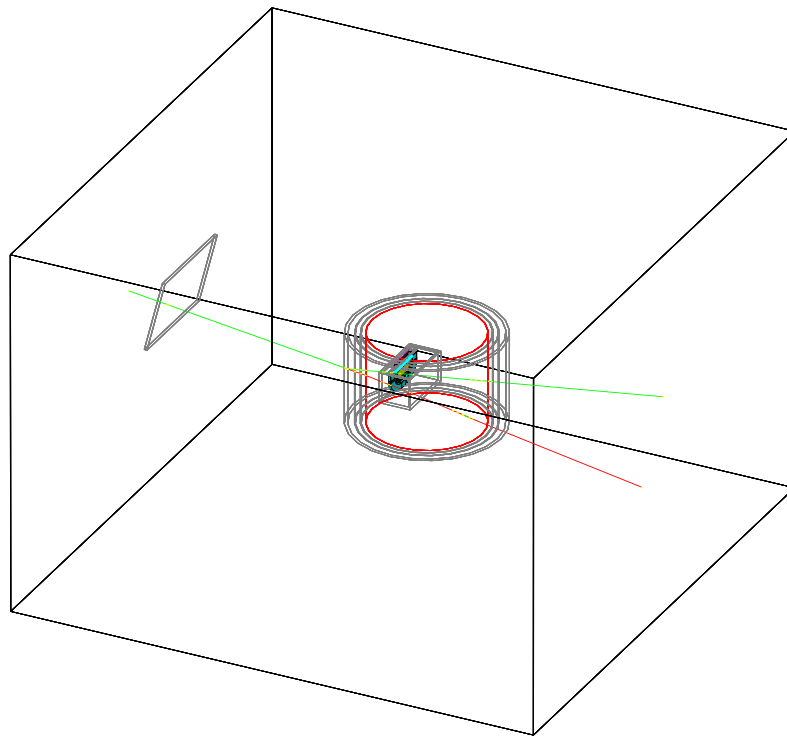


Figure 3: A single PACS high stress module, in the Louvain cyclotron configuration. In gray the single polystyrene foil, the three Al cylinders and the box around the module, in red the Cu cylinder foil.



lowered adding another polystyrene foil<sup>4</sup>. This second one is supposed to be 2.1 mm thick. They calculated the proton energy after the polystyrene layers (last column) using SRIM2000<sup>5</sup>.

### 4.3 The definition of a glitch

A glitch on the photo-conductor is an unexpected voltage jump during the integration ramp. Along a single ramp, that lasts 300 ms, the voltage with a 64 readout sequences decreases monotonically. Whereas the voltage jump overtakes 4 or 6 times (in sigma units) the mean jump that represents a glitch.

The exact electronic behaviour is not reproducible with Geant4, we only collected the energy depositions on the pixels. The energy deposited on the pixels is transformed [1] in Volt following:

$$\Delta E(\text{MeV}) = C\Delta V(\text{Volt})E_g/(e \times g) \quad (1)$$

whereas  $g$  comes out from the photoconductive gain:  $R=\eta g e/(h\nu) = 30 \text{ A/W}$  at  $\lambda=170 \mu\text{m}$  ( $\eta = 0.3$ , with a large error bar).  $E_g$  is the energy gap and it is equal to 2.9 eV and  $C$  is the detector capacity For  $C = 3 \text{ pF}$  we get:  $\Delta V = 0.0134\Delta E$ .

### 4.4 The Geant4 results

We ran the same experiments under the Geant4 tool. For low proton fluxes we ran 5 simulations, in order to have better statistics; for the higher proton fluxes we ran only 2 or 1 simulations. This was done because simulations with high number of primaries are a) time consuming and b) self consisting. Results are summarized in Tab. 3. In Fig. 4 we plot the energy deposition onto the 16 pixels in one of the the N1 tests, in particular the one having the highest number of primaries. G4 results are shown as solid line.

Here we found 4 peaks. The major one, is clearly due the primary proton beaming. The first two, the ones at low energies, are due to the secondary events generated along the tracking of the protons inside the dewar. The peak at higher energy may be explained as follows:

- the pixel are inside a non uniform cavity. Due to the inclination of the beam there is a part of it that cross the cavity in its thinner part, that is pixel are hit by more energetic protons, or
- the initial Gaussian beam is made slightly asymmetric toward higher energies, that is there is a second prominent proton energy that hits the pixels.

## 5 Comparison with measurements

### 5.1 Events and rates

Table 3 reports the simulated outputs on the average number of glitch events and rates for the different measurement setups, while table 4 the measurements of the same quantities. Table 5 compares predicted and measured rates and event numbers for the different instrument setups. Events are defined as described in [1] and [3] at a level of 4 and 6  $\sigma$ . Predicted and measured rates are, within both theoretical and experimental uncertainties, comparable but for high proton energy where the predicted rate is larger by a factor of 4 (as shown also in Figure 4). Theoretical uncertainties are mainly related to unknown instrument setup (see discussion in section 4) and to uncertainties of the physical models. Measurements uncertainties are estimated by the procedure of a glitch definition and the algorithms used to detect a glitch.

<sup>4</sup>Data are available only for N1 and S1 experiments.

<sup>5</sup>SRIM is a SW package which calculates many features of the ion transport in matter, Ziegler, J.F, see <http://www.SRIM.org>.

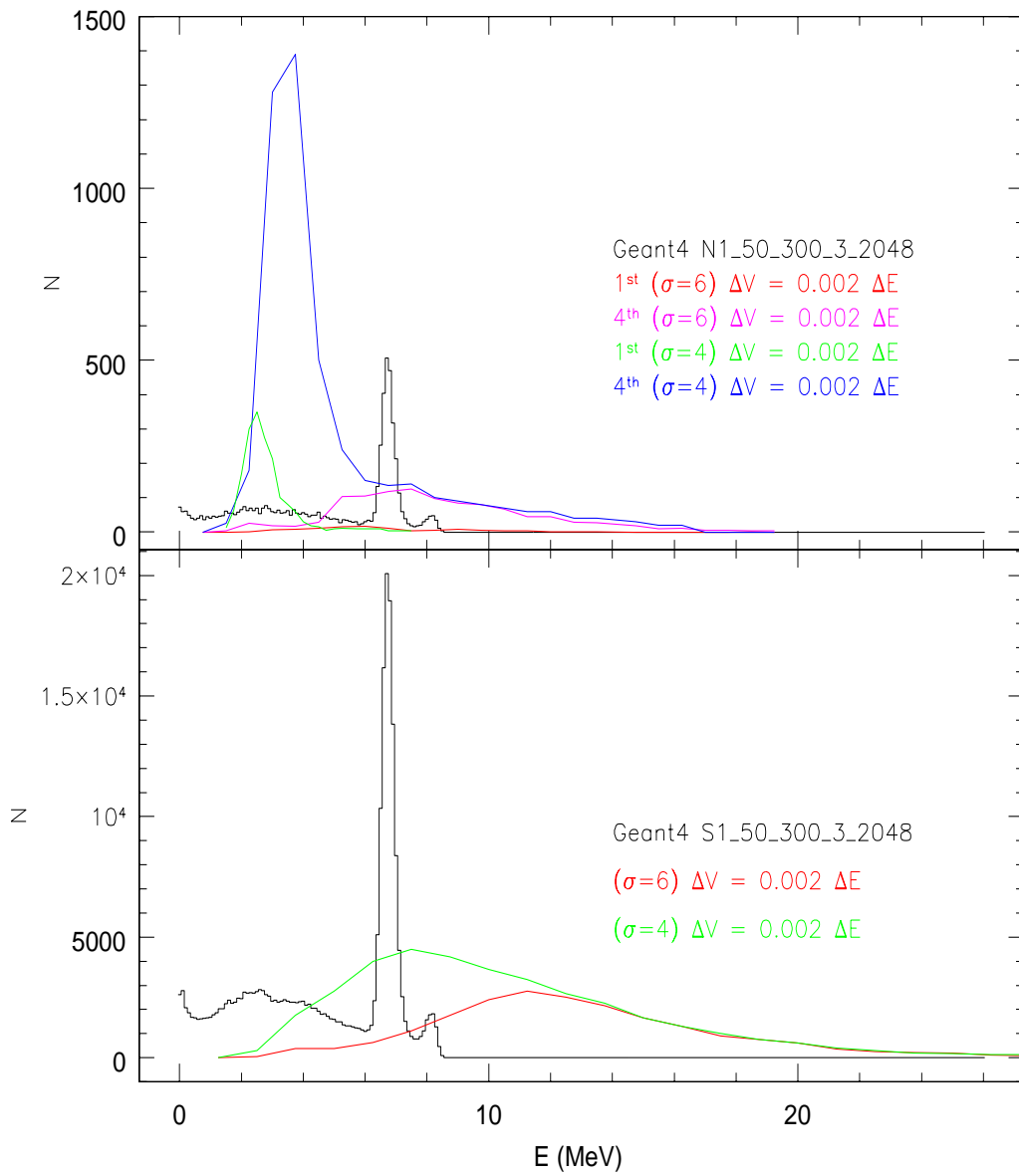


Figure 4: Energy deposition for one of the N1 and S1 tests.

Exp.	$N_{rep}$	$G4_{rep}$	Flux ( $\text{cm}^{-2}\text{s}^{-1}$ )	$t_{rad}$ (s)	$N_p$	$\langle events \rangle$	Rate ( $\text{s}^{-1}\text{cm}^{-2}$ )
#N1	2	10	0.5	38.4	1507	8.10	0.76
	2	10	0.5	38.4	1507	10.10	0.94
	1	5	0.5	38.4	1507	11.00	1.03
	2	10	0.5	256.0	10048	63.60	0.89
	1	5	0.5	153.6	6029	31.60	0.74
	1	5	0.5	307.2	12058	72.18	0.84
	1	5	10.0	153.6	120576	796.20	18.62
44	44	10.0	153.6	120576	766.82	17.93	
40	40	10.0	153.6	120576	755.40	17.67	
5	5	10.0	307.2	241152	1528.80	17.88	
3	6	10.0	614.4	482304	3063.00	17.91	
1	2	10.0	307.2	241152	1534.50	17.94	
2	4	10.0	614.4	482304	2994.75	17.51	
#S1	1	2	400.0	153.6	4823040	29994.50	701.42
	1	2	400.0	150.0	4710000	29760.00	712.64
	14	14	400.0	153.6	4823040	30441.07	711.87
	2	2	400.0	614.4	19292160	121616.00	711.00
	1	2	400.0	204.8	6430720	40704.50	713.91

Table 3: The UCL-CRC experiment outputs with Geant4.

Flux ( $\text{p}/\text{cm}^2/\text{s}$ )	E (MeV)	$\sigma$	$4^{th}$	Events	Time (s)	Rate ( $\text{s}^{-1}\text{cm}^{-2}$ )
10	16.5	6	1	105	1216	0.48
			4	1074	1672	3.61
400			-	20592	1216	95.31
10		4	1	1791	1216	6.08
			4	4469	1672	15.06
400			-	35666	1216	165.06

Table 4: Measured number of events and rates for the first and fourth quarters of the measurements.

## 5.2 Deposited energy

In Figure 4 the distribution of the predicted deposited energy is shown as a black solid line. Color lines correspond to different measurement chunks and different glitch detection thresholds. The number of events increase largely from the first to the last quarter, whatever the detection threshold is set and this effect was explained as due to an increase of detector responsivity ([1]). It has been argued that for a low level cut, as  $4\sigma$ , events which are not strictly glitches may be counted as such and lead to too many fake glitch detections ([1]).

$6\sigma$  threshold events have a peak distribution falling at the same energy as the simulated one, but the distribution shape is completely different, being the simulated one sharp around the value of 7.5 MeV. Furthermore the simulated distribution shows also the secondary effect productions which lack in the measured distribution. This may be due to the cut in the reduction algorithm of the measures glitches. In fact the  $4\sigma$  threshold glitches (shown as a blue and green histogrammes) are accumulated at lower energy (between 2 and 4 MeV) and may be mainly fake glitches.

For higher proton flux (see lower panel) the measured events fall apparently at higher energy. This effect may be due to a change in detector responsivity, i.e. to a different conversion factor between deposited energy and voltage jumps. If this is the case the responsivity may have changed from the N1 to the S1 measurements by a factor of 1.6.

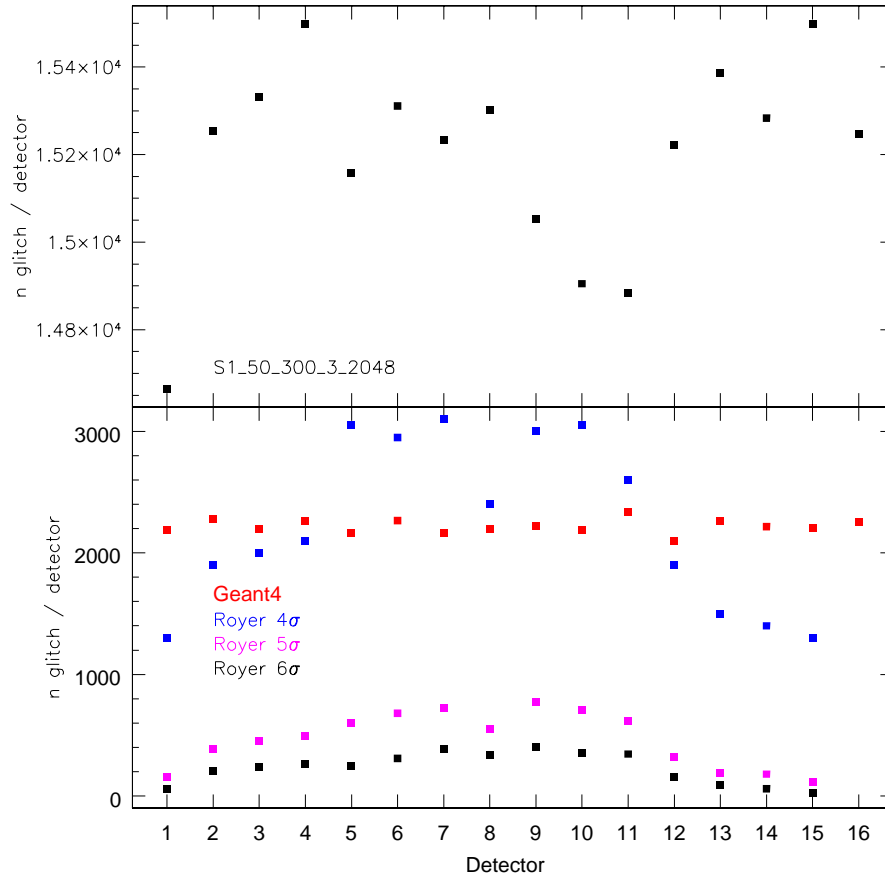


Figure 5: Upper panel: number of Geant4 simulated glitches per detector (pixel) in the S1 setup. Lower panel: number of Geant4 simulated glitches per pixel in the N1 setup are shown as red filled squares. Blue squares correspond to the measured number of glitches/pixel with a  $4\sigma$  threshold (see text for its definition), pink squares to those with a  $5\sigma$  and black to  $6\sigma$  threshold.

### 5.3 Boundary effect

One of the measurement outcomes is a *boundary* effect, i.e. external pixels of the module were under-hit-ted with respect to the central ones. This may be due to the proton beam geometry with a higher concentration of energetic protons in the central part of the circular beam.

Figure 5 reports in the upper panel the number of glitches per pixel for the S1 setup (those with higher proton flux), the lower panel compares the Geant4 results (red filled squares) with the results reported in [3] (see his Fig. 1) (coloured filled squares). Simulations are not able to reproduce this effect. We may explain this an asymmetry of the proton beam which is not reproduced in the simulations.

### 5.4 Cross-talks

We checked whether in the G4 outcomes there are coincidences (“*cross-talks*”) between adjacent pixels. This means that we searched for those events happening in one pixel which then affect also nearby pixels. We find that whenever a pixel is hit-ted the probability that the adjacent one is subsequently hit-ted by the same incoming particle is negligible. Being the flux beamed in a given direction and each pixel is distant from the adjacent one, we do not detect any correlation between hits, i.e. each hit is independent and occurs only in one

Flux (p/cm <sup>2</sup> /s)	E (MeV)	4 <sup>th</sup>	Louvain (6-4σ)		Geant4	
			Events	Rate (s <sup>-1</sup> cm <sup>-2</sup> )	Events	Rate (s <sup>-1</sup> cm <sup>-2</sup> )
0.5	16.5		105-197	0.09 - 3.29	278.4	0.86
10		1	105- 1791	0.48- 6.08	89109.3	17.81
		4	1074- 4469	3.61- 15.06	89109.3	17.81
400		-	20592-35666	95.31-165.06	769865.9	711.32

Table 5: measured versus predicted values.

pixel. In addition in vacuum the produced secondary particles have scattering angles similar to those of the primary protons, making their effect on adjacent pixels negligible.

This predicted result is confirmed by the measurements ([3]), since no statistically significant correlation is detected among events occurring in nearby pixels.

## 6 Conclusions

Simulations are able to reproduce the detected event rates and their energy distribution (but for large proton flux), to explain the lack of effects on nearby pixels, but fail to explain the amount of energy deposition on each pixel, the shape of the deposited energy and the *boundary* effect seen in low energy proton irradiation setup.

This discrepancy is explained as following:

- the entire geometry of the DUT, in particular of the foils between the proton source and the pixels (position, physical, chemical and geometrical details) must be known with accuracy for the simulations to be able to reproduce the effects of each material;
- geometry (diameter, incident angle), energy and energy spread of the incoming proton beam are not known with sufficient accuracy.

This means that simulations cannot take into account of the right polystyrene thickness and by in-air tracking: both should lead to a decreasing in the energies deposited. Dewar and module are correctly reconstructed but all the outside world, which has a fundamental role, is not under control.

## References

- [1] Groenewegen M. *UCL-CRC Proton Tests of March 2004: glitch height distribution*, PICC-KL-TN-012, 2005
- [2] Katterloher R., Barl L., & Shubert J., *Test Plan and Procedures for Investigation of Glitch Event Rate during Proton Irradiation (Test Report)*, PACS-ME-TP-009, 2004
- [3] Royer P. *CQM Proton Irradiation Test Analysis*, PICC-KL-TN-011, 2005
- [4] Royer P. *CQM Proton Irradiation Test Noise Evolution*, PICC-KL-TN-013, 2005
- [5] Santin G., *Herschel PACS Photoconductor: Simulation of the Proton Ground tests*, Technical Note, draft 1.